

Purdue University

Purdue e-Pubs

International Refrigeration and Air Conditioning
Conference

School of Mechanical Engineering

2021

Theoretical study of the heat pump performance for simultaneous production of space heating and domestic hot water

Fernando Tello-Oquendo

Escuela Superior Politécnica de Chimborazo

Daniela Vasconez-Nuñez

Escuela Superior Politécnica de Chimborazo

Jose M Corberan

Universitat Politecnica de Valencia, Spain

Emilio Navarro-Peris

Universitat Politecnica de Valencia, Spain, emilio.navarro@iie.upv.es

Follow this and additional works at: <https://docs.lib.purdue.edu/iracc>

Tello-Oquendo, Fernando; Vasconez-Nuñez, Daniela; Corberan, Jose M; and Navarro-Peris, Emilio, "Theoretical study of the heat pump performance for simultaneous production of space heating and domestic hot water" (2021). *International Refrigeration and Air Conditioning Conference*. Paper 2135. <https://docs.lib.purdue.edu/iracc/2135>

This document has been made available through Purdue e-Pubs, a service of the Purdue University Libraries. Please contact epubs@purdue.edu for additional information. Complete proceedings may be acquired in print and on CD-ROM directly from the Ray W. Herrick Laboratories at <https://engineering.purdue.edu/Herrick/Events/orderlit.html>

Theoretical study of the heat pump performance for simultaneous production of space heating and domestic hot water

Fernando M. TELLO-OQUENDO¹, Daniela C. VÁSCONEZ-NÚÑEZ¹, Emilio NAVARRO-PERIS^{2*}, José M. CORBERÁN²

¹Escuela Superior Politécnica de Chimborazo, Grupo de investigación GIDENM - Facultad de Mecánica, Riobamba, Ecuador (+593 988171087, fernando.tello@epoch.edu.ec)

²Instituto Universitario de Investigación en Ingeniería Energética, Universitat Politècnica de València, Valencia, Spain (+34 963 879 120, *emilio.navarro@ie.upv.es)

* Corresponding Author

ABSTRACT

Nowadays, one of the most important challenges in the residential sector is the efficiency improvement of the equipment and systems used for space heating (SH) and domestic hot water (DHW) production. The main objective is to reduce the consumption of fossil fuels and CO₂ emissions in these applications. In this context, heat pumps are an effective technology as an alternative to boilers for SH and DHW production. However, the SH demand has a different temperature level than the DWH demand. Generally, the SH demand has a variable temperature level that depends on the type of distribution system (type of building) and the different climate conditions, while the DHW demand requires the storage of hot water at a temperature above 60 °C to prevent the presence of legionella. On the other hand, the performance of heat pumps deteriorates when working with high condensing temperatures. This paper presents a theoretical study of the performance of an air-to-water heat pump for simultaneous SH and DHW production, where the use of a desuperheater for DHW production and the condenser for SH production are analyzed. The study shows the optimization of the desuperheater capacity for a given SH demand. The performance of the heat pump is analyzed in terms of the COP and the capacities of the condenser and desuperheater. In addition, the heat pump performance was compared with the performance of two heat pumps (SH and DHW) for the same capacity in terms of compressor swept volume and heat exchanger sizes.

1. INTRODUCTION

Most of the energy consumed for space heating and water heating is produced using natural gas and electricity, as inlet energy for boilers. In the case of the European Union, for water heating, most of the energy consumed is natural gas (49.3%) and electricity (19.7%). Renewables counts for 9.9% of energy consumption, petroleum products for 10.6% and derived heat for 9.2%, while a small proportion (1.4%) is still covered by solid fuels. For space heating, the share of fuels in the final consumption is similar. However, renewables counted for 22.1% and petroleum products for 10.6%, as shown in Figure 1.

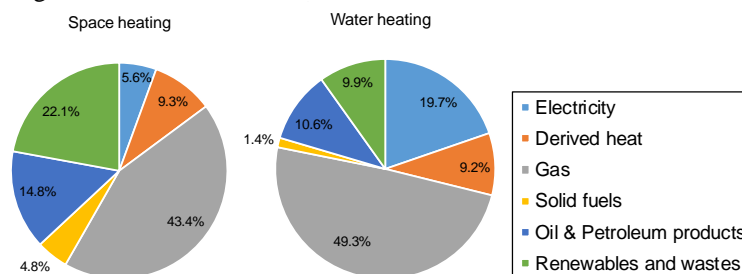


Figure 1: Share of fuels in the final energy consumption in the residential sector by space and water heating, EU-28, 2016 (European Commission, 2018).

In addition, the residential sector mainly uses energy for heating their homes: this represents around two-thirds (64.7%) of their final energy consumption. In addition, the energy used for water heating accounts for 14.5%, meaning that overall, the heating of space and water accounted for 79.2% of the final energy consumed by the residential sector, as shown in Figure 2.

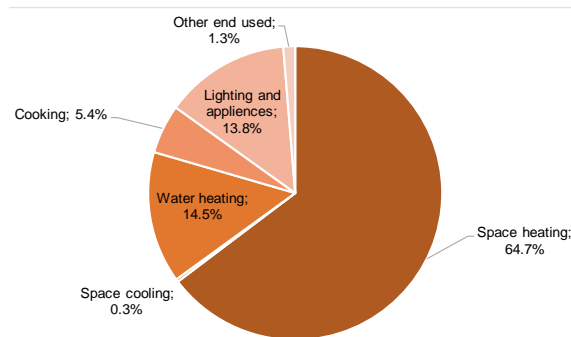


Figure 2: Final energy consumption in the residential sector for each type of end-use, EU-28, 2016 (European Commission, 2018).

For these reasons, the efficiency improvement of the equipment and systems used for space heating (SH) and domestic hot water (DHW) production is one of the most important challenges in the residential sector. The main objective is to reduce fossil fuel consumption and CO₂ emissions in these applications.

In this context, the heat pump is considered an energy-efficient technology for heating and sanitary hot water production. This technology can be an alternative to conventional boilers for SH and DHW production, which use fossil fuels. Hence, applying heat pumps to space heating for residential buildings in cold regions shows the potential of reducing the emissions of greenhouse gases.

However, the SH demand has a different temperature level than the DWH demand. The SH demand has a variable temperature level that depends on the type of distribution system (type of building) and the different climate conditions. On the other hand, the DHW demand requires the storage of hot water at a temperature above 60 °C to prevent the presence of legionella, nevertheless, the performance of heat pumps deteriorates when working with high condensing temperatures.

In general, DHW in residential buildings can be produced by heat pumps in two ways: An individual unit with a relatively low capacity to cover the whole demand or a separate water heater in an integrated unit that simultaneously provides SH. In European markets, the sales of the individual DHW heat pump with an average capacity of 2 to 3 kW has been significantly developing during the past decade. On the other hand, several large-capacity ground-source heat pump units (100 to 400 kW) using HFCs as the refrigerant have been successfully implemented featured with desuperheater in the discharge line, which can provide DHW simultaneously with space heating or cooling (EHPA, 2016). Both solutions are a promising replacement for direct electrical heating in providing DHW, which will save energy in buildings (Xu *et al.*, 2018).

Most of the systems analyzed with simultaneous production of space heating and water heating are water-to-water heat pumps (Fernández-Seara *et al.*, 2012; Sebarchievici & Sarbu, 2015; Blanco *et al.*, 2013); CO₂ heat pump systems (Blanco *et al.*, 2013). Blanco *et al.* (2013) studied a heat pump working with R-410A, with a desuperheater and a condenser, deliberately splitting the gas cooling and the condensation process into two parts. A variable-speed compressor and an electronic expansion valve control the cycle. For a target domestic hot water temperature of 65 °C and space heating temperature of 45 °C, supplied by a ground inlet temperature of 5 °C, the highest COP measured was 4.5. All the previous studies addressed the experimental analysis of the heat pump performance for SH and DHW production, with a specific design. Nevertheless, to our best knowledge, there is no systematic analysis and optimization of this kind of system. Moreover, an important challenge about this application is to optimize the capacity rate, the design, and performance of monovalent heat pump aiming to fulfill the thermal requirements of space heating and water heating in low energy homes according to the demand variation.

In this context, this paper presents a theoretical study of the performance of an air-to-water heat pump for simultaneous SH and DHW production, where the use of a desuperheater for DHW production and the condenser for SH production

are analyzed. The study shows the optimization of the desuperheater capacity for a given SH demand. The performance of the heat pump is analyzed in terms of the COP and the capacities of the condenser and desuperheater. In addition, in this paper, the authors compare the performance of the heat pump for simultaneous production of SH and DHW with the performance of two heat pumps for SH and DHW production, separately.

2. METHODOLOGY

In order to study the performance of the heat pump, a general model of the vapor compression cycle was implemented using EES software (Klein & Alvarado, 2017). The boundary conditions of the cycle are evaporating temperature, condensing temperature, superheat at the compressor inlet, and subcooling at the condenser outlet.

The evaporator mass flow rate is determined by Equation (1), where the number 1 is located at the compressor inlet, ρ represents the density in (kg/m^3), η_v represents its volumetric efficiency, \dot{V}_s is the swept volume of the compressor in (m^3/s). The volumetric efficiency of the compressor is modeled as a linear correlation in terms of the pressure ratio (Pr) determined by Equation (2). All points are referred to the schematic of the cycle in Figure 3.

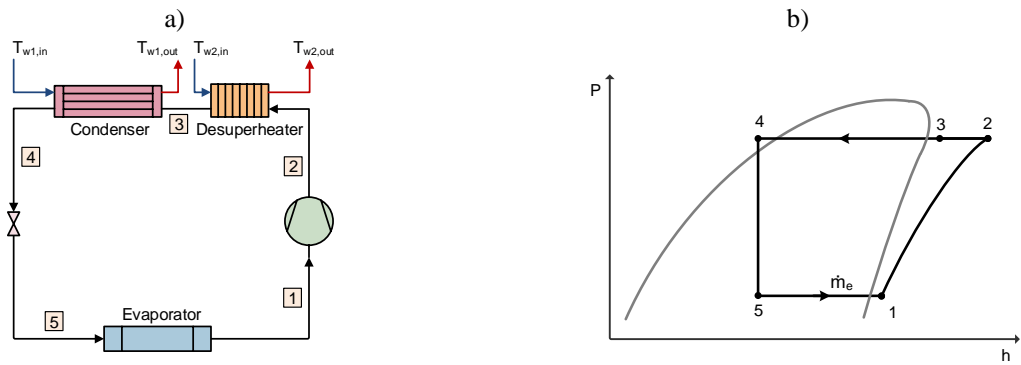


Figure 3: a) Scheme of the heat pump for simultaneous production of space heating and domestic hot water. b) P-h diagram of the cycle.

$$\dot{m}_e = \eta_v \dot{V}_s \rho_1 \quad (1)$$

$$\eta_v = A_1 * P_r + B_1 \quad (2)$$

$$T_1 = T_e + SH \quad (3)$$

$$T_4 = T_c - SC \quad (4)$$

The refrigerant properties at the evaporator outlet (point 1) are defined by the evaporating temperature (T_e) and the superheat at the compressor inlet (SH) by Equation (3). The refrigerant properties at the condenser outlet (point 4) are defined by the condensing pressure and the subcooling (Equation (4)).

The compressor efficiency is calculated by Equation (5) as a function of the pressure ratio. The coefficients of the compressor efficiencies correlations (Equations (2) and (3)), were fitted based on catalog data of a scroll compressor of $14.269 \text{ m}^3/\text{h}$.

$$\eta_c = A_2 \left[1 - \exp\left(-\frac{P_r - D_2}{B_2}\right) \right] - C_2 \ln(P_r + 1) \quad (5)$$

All thermophysical properties of the refrigerant at the different points are calculated with the NIST REFPROP database (Lemmon *et al.*, 2010). The model neglects the pressure drop in the heat exchangers and considers an isenthalpic expansion in the valve.

The desuperheater (DSH) is modeled by using an ε -Ntu approach, considering counter-flow between the refrigerant and the secondary fluid (water). The heat exchanged in the DSH is calculated by Equation (6), where \dot{C}_{min} is the minimum capacitance rate of the fluids, the effectiveness (ε) is calculated by Equation (7) and the NTU by Equation (8). The conductance UA is a parameter of the model in (W/K).

$$\dot{Q}_{DSH} = \varepsilon * \dot{C}_{min} * (T_2 - T_{w2,in}) \quad (6)$$

$$\varepsilon = f(\dot{C}_{ref}, \dot{C}_w, Ntu) \quad (7)$$

$$Ntu = \frac{UA}{\dot{C}_{min}} \quad (8)$$

When the refrigerant state at the desuperheater outlet (point 3) is in superheat condition, the condensing temperature is defined by the energy balance in the condenser. Hence, the condensing temperature is limited by the temperature profile of the secondary fluid through an internal pinch point as shown in Figure 4.

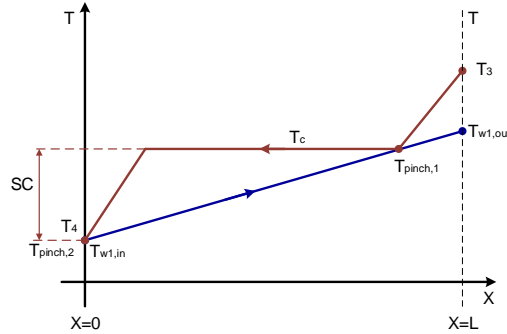


Figure 4: Temperature profile of the water and refrigerant into the condenser.

Therefore, the following energy balance is posed in the condenser.

$$\dot{m}_{w1} C_{p_{w1}} (T_{w1,out} - T_{w1,in}) = \dot{m}_e (h_3 - h_4) \quad (9)$$

$$\dot{m}_{w1} C_{p_{w1}} (T_{pinch,1} - T_{w1,in}) = \dot{m}_e (h_{pinch,1} - h_4) \quad (10)$$

$$T_{pinch,1} = T_c \quad (11)$$

The enthalpy at the condenser outlet is defined by Equation (12). The temperature approach in the condenser with infinite heat transfer area (Equation (13)) is equal to 0 K.

$$h_4 = h(P_c, T_b(P_c) - SC) \quad (12)$$

$$DT_{pinch,2} = T_4 - T_{w1,in} \quad (13)$$

The compressor power consumption (\dot{E}) is estimated from the overall compressor efficiency definition, using Equation (14).

$$\dot{E} = \frac{\dot{m}_e (h_{2s} - h_1)}{\eta_c} \quad (14)$$

The capacity destined for domestic water heating (desuperheater capacity) is defined by Equation (15), and the capacity destined for space heating (condenser capacity) is defined by Equation (16). The heating COP of the heat pump is defined by Equation (17).

$$\dot{Q}_{DHW} = \dot{m}_{w2} C_{p_{w2}} (T_{w2,out} - T_{w2,in}) \quad (15)$$

$$\dot{Q}_{SH} = \dot{m}_{w1} C_{p_{w1}} (T_{w1,out} - T_{w1,in}) \quad (16)$$

$$COP = \frac{\dot{Q}_{DHW} + \dot{Q}_{SH}}{\dot{E}} \quad (17)$$

For the cycle simulations, the parameters showed in Table 1 are defined.

Table 1: Parameters defined for cycle simulations.

Parameter	Value
Refrigerant	R-290
\dot{V}_s	14.269 m ³ /h
T_e	-8 °C
SH	5 K
$T_{w1,in}$	40 °C
$T_{w1,out}$	45 °C
$T_{w2,in}$	10 °C
$T_{w2,out}$	60 °C

Considering that the heat pump is designed to meet the space heating demand, this paper aims to analyze how much capacity can be extracted to heat water using a desuperheater before the condenser. The heat pump analyzed has two thermal sinks with different temperature levels and temperature lifts. For the DWH, the desuperheater has a high-temperature lift (50 K) and a high-temperature level (60 °C). For the SH, the condenser has a small temperature lift (5 K) and a low-temperature level (45 °C). In this context, the temperature of the heat sink in both the condenser and in the desuperheater has no constant temperature. Hence, the definition used in Equation (16) to estimate the cycle COP, considering as reference the ideal Carnot cycle, is not the best way to estimate the cycle performance. Therefore, in order to analyze the cycle performance when the heat sink has a temperature lift, the ideal Lorenz cycle is considered as a reference. Hence, the Coefficient of Performance of Lorenz (Hasan *et al.*, 2002) is defined for each heat sink, by Equations (18) and (19).

$$COP_{L,1} = \frac{\overline{T_{H,1}}}{\overline{T_{H,1}} - \overline{T_{C,1}}} \quad (18)$$

$$COP_{L,2} = \frac{\overline{T_{H,2}}}{\overline{T_{H,2}} - \overline{T_{C,2}}} \quad (19)$$

Where $\overline{T_{H,i}}$ is the logarithmic mean temperature of the heat sink and $\overline{T_{C,i}}$ is the logarithmic mean temperature of the heat source. In this case, the $\overline{T_{C,i}} = T_e$ because the evaporating temperature is considered constant.

$$\overline{T_{H,1}} = \frac{T_{w1,in} - T_{w1,out}}{\ln\left(\frac{T_{w1,in}}{T_{w1,out}}\right)} \quad (20)$$

$$\overline{T_{H,2}} = \frac{T_{w2,in} - T_{w2,out}}{\ln\left(\frac{T_{w2,in}}{T_{w2,out}}\right)} \quad (21)$$

Since the cycle has two heat sinks and each heat sink has its respective capacity, it is necessary to define a Weighted Lorenz COP (\overline{COP}_L) for the cycle using the Equation (22). This factor is the sum of the product of each $COP_{L,i}$ by the capacity ratio (α_i) of each heat sink defined in Equations (23) and (24).

$$\overline{COP}_L = \alpha_1 COP_{L,1} + \alpha_2 COP_{L,2} \quad (22)$$

$$\alpha_1 = \frac{\dot{Q}_{SH}}{\dot{Q}_{SH} + \dot{Q}_{DHW}} \quad (23)$$

$$\alpha_2 = \frac{\dot{Q}_{DHW}}{\dot{Q}_{SH} + \dot{Q}_{DHW}} \quad (24)$$

Finally, based on a second law analysis, the Weighted Lorenz Efficiency is defined by Equation (25). This efficiency relates the cycle COP with the Weighted Lorenz COP of the cycle.

$$\eta_L = \frac{COP}{\overline{COP}_L} \quad (25)$$

In order to analyze the capacities of the condenser and the desuperheater, a parametric study is performed for several values of water mass flow rate through the desuperheater (\dot{m}_{w2}), which is varied from 0.0001 to 0.0475 kg/s.

3.- RESULTS AND DISCUSSION

Figure 5a shows the variation of the SH and DHW capacity as a function of the water mass flow rate through the desuperheater (\dot{m}_{w2}). As the water mass flow rate through the desuperheater increases, the capacity destined for the SH decreases linearly. With these results, an optimal capacity ratio cannot be established for the simultaneous production of SH and DHW. Figure 5b depicts the variation of the COP and the condensing temperature as a function of the flow of water through the desuperheater

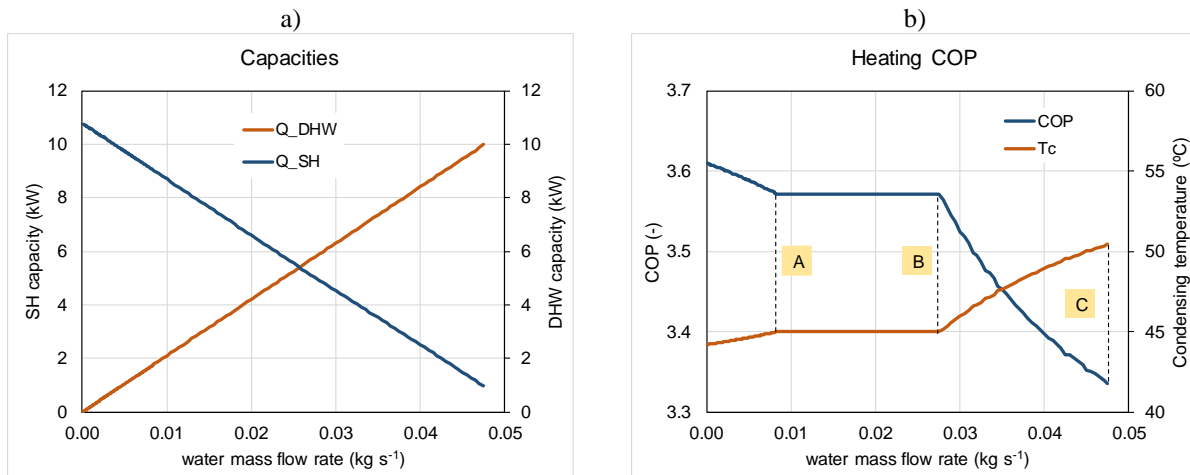


Figure 5: a) Variation of the heating capacity for SH and DHW production as a function of the water mass flow rate through the desuperheater. b) Variation of the COP and condensing temperature as a function of the water mass flow rate through the desuperheater.

Figure 5b shows that the COP and the T_c vary in three phases. The first phase corresponds from 0.0001 to 0.008298 kg/s, up to the condition “A”. In this range, the refrigerant at the desuperheater outlet (see point 3 in Figure 3a) is in superheat condition. Therefore, the condensing temperature is defined by the energy balance in the condenser, and it is limited by the temperature profile of the secondary fluid, as can be seen in Figure 4. Hence the lower T_c , which maximizes the COP, is achieved when there are two pinch points equal to zero in the condenser. During this first phase, the condensing temperature increases smoothly and the COP decreases.

As the \dot{m}_{w2} increases, the refrigerant achieves the condition “A”. In this condition, point 3 is in a saturated state, as shown in Figure 6. Hence, the lower value of T_c is equal to the outlet temperature of the water in the condenser ($T_c = T_{w1,out} = 45$ °C), to avoid temperature crossings and fulfill the second law of thermodynamics.

a)

b)

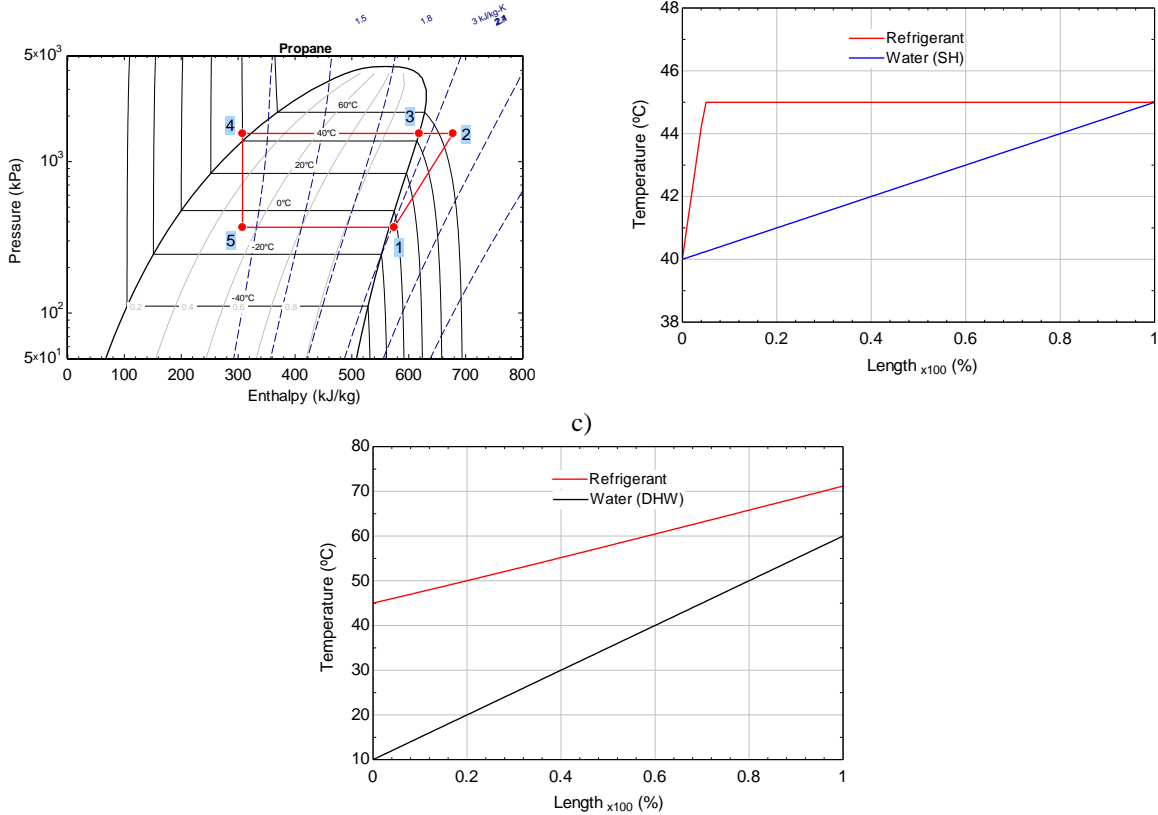
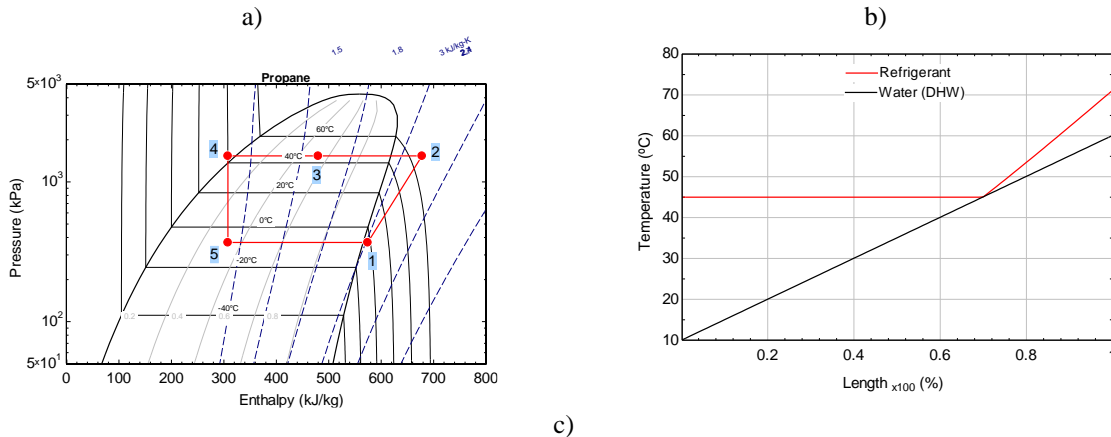


Figure 6: a) P-h diagram of the cycle when point 3 is in a saturated state. Condition “A”. b) Temperature profile of the condenser. c) Temperature profile of the desuperheater.

After this point, the second phase is when point 3 is in biphasic condition, for \dot{m}_{w2} values from 0.008298 kg/s to 0.0275 kg/s. In this range, the T_c is also determined by the energy balance in the condenser. Therefore, the T_c and COP remain constants up to the condition “B” (see Figure 5b). The condition “B” is achieved when the internal pinch point in the desuperheater is equal to zero, as shown in Figure 7b. This is the thermal limit in the heat exchanger of an infinite heat transfer area. Hence, the $T_c=45^\circ\text{C}$ and the temperature profile of the condenser are the same as in Figure 6b. After condition “B”, in the third phase, the condensing temperature is determined by the energy balance in the desuperheater. Due to the \dot{m}_{w2} increases from 0.0275 to 0.04575 kg/s, the T_c must increase in order to supply the necessary energy to heat the desuperheater water, maintaining the internal pinch point. Therefore, point 3 remains in biphasic condition up to the condition “C” that corresponds to the bubble point (saturated liquid).



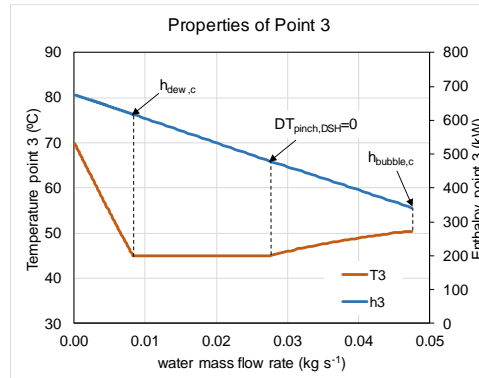


Figure 7: a) P-h diagram of the cycle when point 3 is in a saturated state. Condition “B”. b) Temperature profile of the desuperheater. c) Refrigerant thermal properties of point 3 as a function of the mass flow rate in the desuperheater.

Because the T_c increases in this third phase, the cycle COP is affected and decreased up to 3.572. In order to illustrate the variation of the refrigerant properties of point 3, its enthalpy and temperature are plotted in Figure 7c.

Nevertheless, with the variables analyzed previously, it is not possible to find an optimal operating condition for this heat pump. As commented in section 2, the cycle has to be studied considering the Weighted Lorentz COP (\overline{COP}_L) and the Weighted Lorentz Efficiency (η_L). Figure 8a shows the COP_L for SH and DHW. The $COP_{L,1}$ for SH is lower than the $COP_{L,2}$ for DHW, because the temperature level and the temperature lift in the secondary fluid of the desuperheater are higher. Therefore, the heat pump can work between two bands of Lorentz's COP, that of SH ($COP_{L,1}$) and that of DHW ($COP_{L,2}$). The heat pump operation is represented by the \overline{COP}_L factor. When the water mass flow rate through the desuperheater (\dot{m}_{w2}) is zero, the heat pump works only for SH and the \overline{COP}_L is equal to the $COP_{L,1}$. As the \dot{m}_{w2} increases, the \overline{COP}_L increases until it reaches $COP_{L,2}$ at condition “C”. This behavior indicates that the higher the \dot{m}_{w2} , the higher the \overline{COP}_L . However, from condition “B”, the T_c increases, causing the dropping of the system COP due to the compressor power input increasing with T_c . This variation in system performance is analyzed with the Lorentz weighted efficiency (η_L). Note that condition “B” is achieved when there is an internal pinch point equal to zero in the desuperheater. In this condition, the T_c has the lowest value (45 °C).

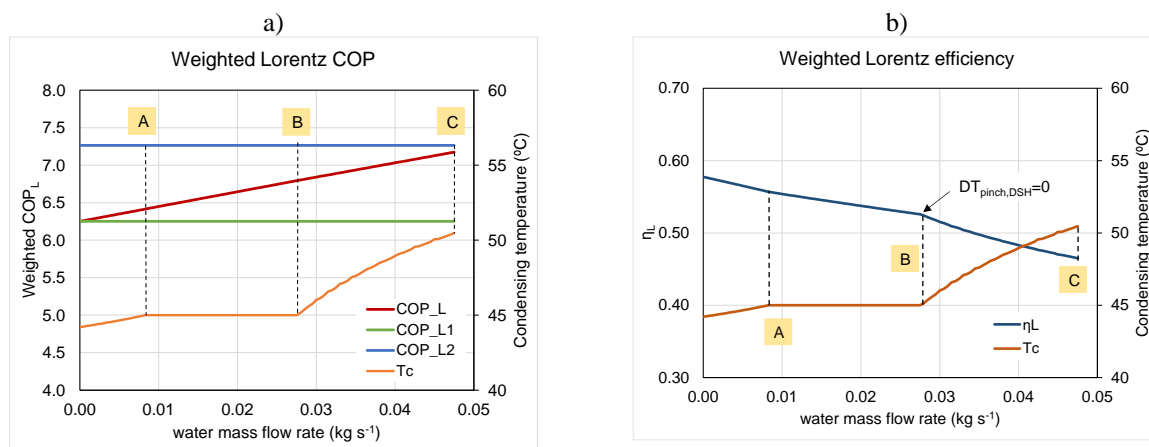


Figure 8: Variation of the Weighted Lorentz Efficiency as a function of the mass flow rate in the desuperheater.

Figure 8b illustrates the variation of the η_L as a function of the \dot{m}_{w2} . At condition “B”, an inflection point of the η_L is evident, from which the η_L drops significantly. Consequently, condition “B” is a reference point for the design of heat pumps for simultaneous production of SH and DHW and for optimizing the desuperheater capacity. At that condition, the highest possible DHW capacity is achieved before the COP of the system falls due to the increase of T_c .

In order to compare the performance of the heat pump for simultaneous production of SH and DHW with the case of producing SH and DHW with two heat pumps separately, the performance of the two heat pumps was calculated considering the same capacities of SH and DHW. The results are summarized in Table 2.

Table 2. Operating conditions of the heat pump for the production of SH and DHW simultaneously and separately for an evaporating temperature of -8°C .

Parameter	Heat pump for simultaneous production of SH and DHW		Heat pump for SH	Heat pump for DHW
	Condenser	Desuperheater	Condenser	Condenser
$T_{w,in}$ ($^{\circ}\text{C}$)	40	10	40	10
$T_{w,out}$ ($^{\circ}\text{C}$)	45	60	45	60
\dot{m}_w (kg/s)	0.2409	0.0275	0.2406	0.02757
\dot{m}_a (kg/s)	0.0292		0.01364	0.01239
\dot{Q} (kW)	5.028	5.782	5.028	5.782
\dot{E} (kW)	3.026		1.393	1.466
$\text{COP} \left(\frac{\dot{Q}_{SH} + \dot{Q}_{DHW}}{\dot{E}} \right)$	3.572		3.610	3.945
$\text{COP} \left(\frac{\dot{Q}_{SH} + \dot{Q}_{DHW}}{\dot{E}_{SH} + \dot{E}_{DHW}} \right)$	-		3.781	
COP_L	6.251	7.2650	6.251	7.265
α (-)	0.465	0.535	0.465	0.535
$A_{\text{heat exchanger}}$ (m^2)	0.92	0.71	1.43	0.92
$\overline{\text{COP}}_L$	6.794		6.793	
η_L	0.526		0.557	
\dot{V}_s	14.269		6.652	6.182

As expected, the compressor size of the heat pumps for SH and DHW separately is smaller than the compressor size needed for the simultaneous production of SH and DHW. Separate heat pumps achieve 5.85% higher combined COP and 5.89% better Lorentz Weighted Efficiency than the heat pump of simultaneous production of SH and DHW.

The SH condenser of the separate heat pump has a 55% greater heat exchange area than the condenser of the simultaneous production heat pump. This is because the refrigerant in the simultaneous SH condenser does not have the desuperheat phase.

It is important to note that, the heat pump will work continuously to satisfy the SH demand, and, when necessary, the heat pump will operate to satisfy simultaneously both the SH and DHW demand. When it occurs, the system has to work in the obtained conditions to achieve optimum performance. The hot water is stored in a tank.

Once identified the optimum conditions, the designers can size the desuperheater to achieve these optimum conditions.

4.- CONCLUSIONS

This paper presents a theoretical study of the performance of an air-to-water heat pump for simultaneous SH and DHW production, where the use of a desuperheater for DHW production and the condenser for SH production are analyzed. The following conclusions can be drawn from this study:

- The best operating condition of the heat pump for simultaneous SH and DHW production is achieved when having an internal pinch point equal to zero in the desuperheater.
- For the given application, the capacity of DHW production is 1.15 the capacity of SH.
- As the water mass flow rate increases, the cycle COP always decreases. Hence, the COP is not useful to analyze the real cycle performance because the proposed application does not have secondary fluid with a constant temperature.
- A weighted Lorentz efficiency was defined to study cycle performance. This efficiency relates the cycle COP with the weighted Lorentz COP, considering the temperature level and temperature lift of the two heat sinks.
- In the best operating condition, the condensing temperature is determined by the energy balance in the desuperheater, and it is limited by the temperature profile into the heat exchanger.
- The combined COP of the production of SH and DHW with separate heat pumps is 5.85% better than the COP of the heat pump for simultaneous production of SH and DHW.

- The weighted Lorentz efficiency of the production of SH and DHW with separate heat pumps is 5.89% better than the weighted Lorentz efficiency of the heat pump for simultaneous production of SH and DHW.
- The condenser heat transfer area for the heat pump for simultaneous production of SH and DHW is 55% lower than the condenser heat transfer area for the separate heat pump for SH.
- The results presented in this study are useful to optimize the operation when the heat pump produces simultaneously SH and DHW. Moreover, the study provides information to size the desuperheater in order to maximize the DHW capacity for a given SH demand.

NOMENCLATURE

A	heat transfer area	(m ²)	Subscript	
\dot{E}	compressor consumption	(kW)	c	condenser
COP	coefficient of performance	(-)	DHW	domestic hot water
COP _L	Lorentz COP	(-)	e	evaporator
h	enthalpy	(kJ/kg)	SH	space heating
\dot{m}	mass flow rate	(kg/s)	w	water
P	pressure	(kPa)	Greek symbols	
Pr	pressure ratio	(-)	ρ	density (kg/m ³)
\dot{Q}	capacity	(kW)	η_c	overall compressor efficiency (-)
SC	subcooling	(K)	η_v	volumetric efficiency (-)
SH	superheat	(K)	η_L	weighted Lorentz efficiency (-)
T	temperature	(°C)		
\dot{V}_s	swept volume	(m ³ /s)		

REFERENCES

- Blanco, D. L., Nagano, K., & Morimoto, M. (2013). Experimental study on a monovalent inverter-driven water-to-water heat pump with a desuperheater for low energy houses. *Appl. Therm. Eng.*, 50, 826-836.
- EHPA. (2016). *European Heat Pump Market and Statistics Report 2016*. Brussels-Belgium: European Commission 7th framework program. Next Generation of Heat Pumps working with Natural fluids.
- European Commission. (2018). *Eurostat. Statistics Explained - Energy consumption in households*. Recuperado el 04 de 12 de 2018, de https://ec.europa.eu/eurostat/statistics-explained/index.php?title=Energy_consumption_in_households
- Fernández-Seara, J., Pereiro, A., Bastos, S., & Dopazo, J. A. (2012). Experimental evaluation of a geothermal heat pump for space heating and domestic hot water simultaneous production. *Renew. Energ.*, 48, 482-488.
- Hasan, A. A., Goswami, D. Y., & Vijayaraghavan, S. (2002). FIRST AND SECOND LAW ANALYSIS OF A NEW POWER AND REFRIGERATION THERMODYNAMIC CYCLE USING A SOLAR HEAT SOURCE. *Sol. Energy*, 73(5), 385-393.
- Klein, S. A., & Alvarado, F. L. (2017). EES-Engineering Equation Solver. Academic Professional Version 10.091. F-Chart Software. Madison, WI.
- Lemmon, E., Huber, M., & Mc Linden, M. (2010). *NIST Standard Reference Database 23:Reference Fluid Thermodynamic and Transport Properties-refprop. Version 9.0*. Gaithersburg: National Institute of Standards and Technology, Standard Reference Data Program.
- Sebarchievici, C., & Sarbu, I. (2015). Performance of an experimental ground-coupled heat pump system for heating, cooling and domestic hot-water operation. *Renew. Energ.*, 76, 148-159.
- Stene, J. (2005). Residential CO2 heat pump system for combined space heating and hot water heating. *Int. J. Refrig.*, 28, 1259-1265.
- Xu, T., Navarro-Peris, E., Piscopiello, S., Sawalha, S., Corberán, J. M., & Palm, B. (2018). LARGE-CAPACITY PROPANE HEAT PUMPS FOR DHW PRODUCTION IN RESIDENTIAL BUILDINGS. In Commissions B1, B2, E1, & E2 (Eds.). *Proceedings of the 13th IIR Gustav Lorentzen Conference on Natural Working Fluids, Valencia-Spain*. Paris, France: IIF/IIR